Ocular effects of argon laser radiation
I. Retinal damage threshold studies

George H. Bresnick, Georg D. Frisch, James O. Powell, Maurice B. Landers, Gerald C. Holst, and Alexander G. Dallas

The eyes of Rhesus monkeys were exposed to an argon laser operating at 5,145 Å. Retinal exposure sites were examined with ophthalmoscopic and histopathologic techniques. The retinal damage threshold was determined ophthalmoscopically for exposure durations of 12, 70, 125, and 1,000 msec. The utilization of flat preparations of the pigment epithelium and sensory layers of the retina proved to be a more sensitive method for evaluating threshold retinal damage.

Key words: retina, retinal pigment epithelium, retinal damage threshold, retinal histology, retinal flat-preparation, argon laser, laser safety, Rhesus monkey, probit analysis, laser hazard.

This paper describes a combined ophthalmoscopic and histologic investigation of the threshold of retinal injury from the argon laser. In previous reports on the argon laser[1-3] the retinal injury threshold has been defined in terms of the minimal laser energy required to produce an ophthalmoscopically visible retinal lesion. In studies with other laser systems,[4-6] however, investigators have shown by histologic methods that retinal damage may be produced at energy levels below the ophthalmoscopically determined threshold. Therefore, in the present study we have employed both ophthalmoscopic and histologic criteria of damage. We have designed the experiment to permit statistical analysis of the results from both techniques.

The Joint AMRDC-AMC Laser Safety Team, Frankford Arsenal, Philadelphia, Pa.

Manuscript submitted Aug. 11, 1970; manuscript accepted Sept. 2, 1970.

Materials and methods

The laser exposure facility (Fig. 1) consisted of a Spectra-Physics Induction Ion Laser, Model 140, which produced approximately 900 milliwatts (mw.) at 5,145 Å in a transverse electromagnetic mode (TEM_{00}). The beam diameter was 1.6 mm. with a beam divergence of 0.7 milliradians.

A portion of the raw beam was deflected onto an EG&G Lite Mike, Model 560B, for a continuous sampling of the output during the course of the experiment. Exposure durations of 12, 70, 125, and 1,000 msec. were obtained by using an electrically activated shutter. The beam was attenuated to the desired power level by introducing calibrated neutral density filters. The attenuated beam was split by a multilayered dielectric coated beam splitter (56 per cent transmission and 44 per cent reflection at 45°) for 12, 70, and 125 msec. exposures and by a pellicle (68 per cent transmission and 32 per cent reflection at 45°) for the 1,000 msec. exposures. A low-power aiming light was produced by opening the shutter and leaving a filter of optical density 3 in the path of the beam.

Monitoring of the beam was accomplished with the use of a primary and secondary detector, each composed of a diffusion block and solar

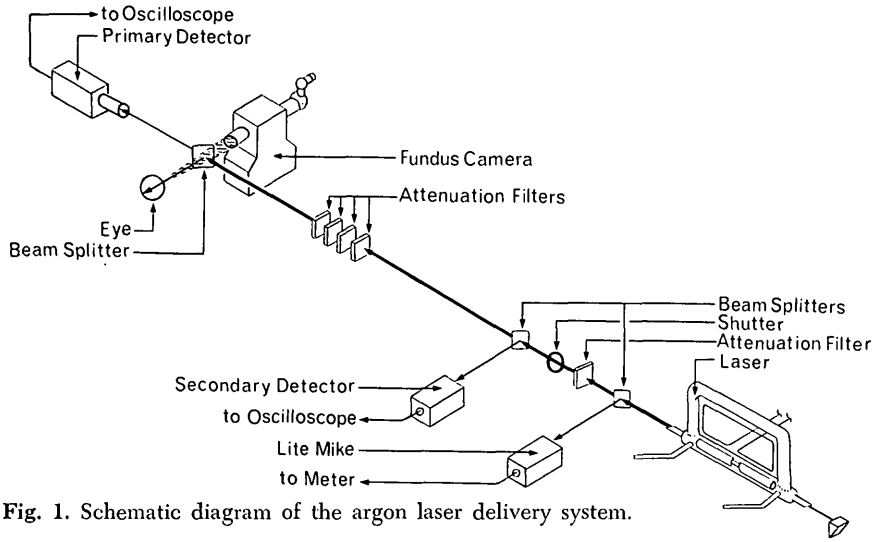

Fig. 1. Schematic diagram of the argon laser delivery system.

cell. The power recorded by the primary detector was used to determine the power delivered to the eye of the animal by applying the calibration of the beam splitter. The secondary detector sampled the unattenuated beam. The primary detector was calibrated to a TRG Ballistic Thermopile, Model 100. The secondary detector was not absolutely calibrated outside of checking its linearity in the region used because it served only as a normalizing device to correlate one exposure to another.

Rhesus monkeys *(Macaca mulatta)* weighing between 2 and 5 kilograms were preanesthetized with a sedative dose of phencyclidine hydrochloride (0.25 mg. per kilogram) intramuscularly and atropine sulfate (0.2 mg.) subcutaneously. Anesthesia was induced with sodium pentobarbital (approximately 5 mg. per kilogram) via the saphenous vein, through a pediatric intravenous injection set, which also was used to administer fluids and additional anesthetic during the course of the experiment. The pupils were dilated with phenylephrine hydrochloride (10 per cent) and cyclopentolate hydrochloride (1 per cent). Sutures were placed in the upper eyelids to facilitate manipulation. The animals were refracted while under anesthesia, using a Copeland streak retinoscope, and appropriate correcting lenses were placed in the path of the beam. During the course of the experiment, corneal transparency was maintained by frequent irrigation of the eye with physiologic saline.

An estimate of the size of the retinal spot produced by the argon laser was made in the following manner: a stainless steel wire of known diameter was introduced through a sclerotomy site at the level of the pars plana, and the wire was guided under observation by indirect ophthalmoscopy onto the retinal surface at the posterior pole; the argon aiming light and wire were then photographed simultaneously and the relative diameters were measured. Calculations showed the diameter of the retinal spot to be approximately 40 to 50 μ.

During laser exposure the animal was restrained in a holder which allowed precise rotation around the geometric center of the animal's cornea. The device permitted a displacement of 30° above and below the horizontal plane, as well as 30° to the left and right of the vertical plane. The animal holder rode on an optical bench placed perpendicularly to the main optical bench to allow viewing of the fundus with a Zeiss Fundus Camera.

The laser beam was directed through the central 3 mm. of the cornea. Twenty-four laser exposures were placed in a grid pattern at the posterior pole of each eye. The top row consisted of six gross "marker" lesions with the remaining exposures located in columns of three below each marker. The technique facilitated the localization of each exposure site during the ophthalmoscopic and histologic evaluations.

All sites were examined through a fundus camera at 5, 10, and 15 minutes following exposure, and with a direct ophthalmoscope at 30 and 60 minutes. Some lesions did not appear until 15 minutes after exposure. No difference was noted between endpoints of 30 and 60 minutes. A positive result was taken to be an ophthalmoscopically visible lesion present 60 minutes after exposure. No attempt was made to separate the results of macular from extramacular exposures.

Histopathologic examination was performed on a random sample of eyes for the 12 and 125 msec, exposure durations. The animals were killed

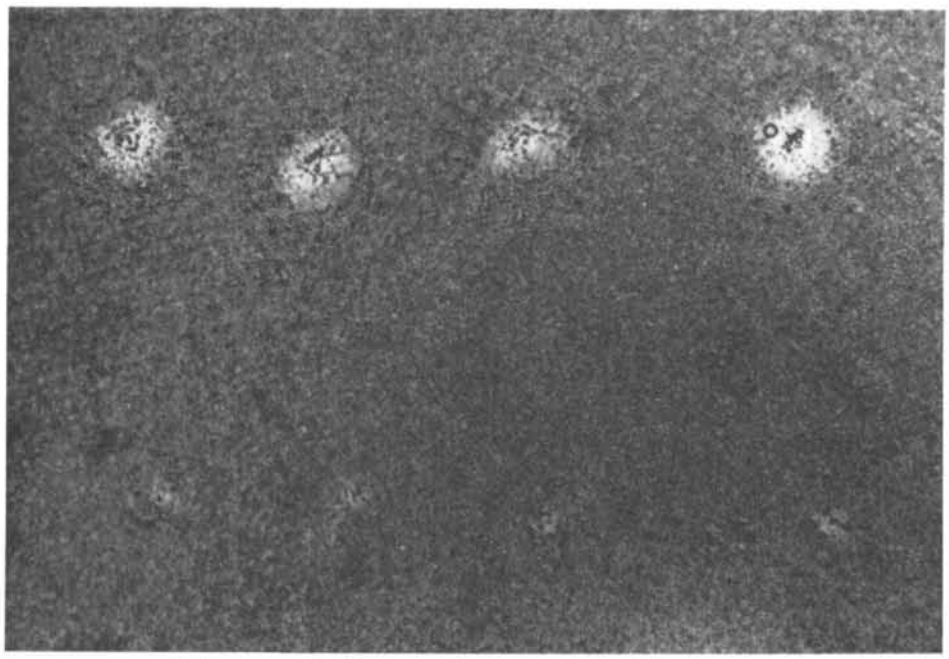

Fig. 2. Unstained flat-mount of Rhesus monkey pigment epithelium and sensory retina. The upper row of large lesions are "marker" lesions, placed to facilitate the localization of exposure sites. The lower row contains threshold lesions (Argon laser: 5,145 Å, 10 to 18 mw., 125 msec.). (×300.)

from one to ten days following laser exposure as previously described.[7] Following enucleation either unstained flat-mounts of the pigment epithelium and sensory layers of the retina or serial sections of paraffin-embedded specimens (6 to 8 μ thick) stained with hematoxylin and eosin were prepared and examined by light microscopy.

The technique for preparing whole flat-mounts of the retina and pigment epithelium afforded an expedient method for examining a large number of exposure sites (Fig. 2). In contrast, the use of serial sections proved to be quite time consuming, and there was considerable uncertainty in reliably identifying exposure sites. The quantitative data from the flat-preparations only, therefore, were included in the results, along with a qualitative description of the morphology of the laser lesions by both methods.

The data were evaluated by several methods, and the results were compared for agreement and consistency. Most previous reports of laser threshold studies employed *histograms* for data analysis. The histograms were prepared by dividing the dose range into equal increments, calculating the proportion of damage within each increment, and constructing one or more step-functions. Probability curves were drawn which visually fitted the step-functions best. There are some inherent problems with this technique. First of all, there is the difficulty in confidently choosing the best visual fit. Secondly, determining the dose level at which the histogram meets the zero or 100 per cent level of damage requires a very extensive experiment based on a large number of test sites.

In addition to using histograms, therefore, we also evaluated the data by probit methods of analysis: the *graphical probit method* and the *computational (exact) probit method.* These methods have been specifically developed to handle quantal response data. The graphical method[8] is the simpler of the two. It gives the median effective dose (ED_{50}), the slope of the regression line, and the associated confidence intervals (CI). The use of logarithmic-probability paper permits plotting the data in original units and eliminates the problem of converting log-probit equations to their arithmetic equivalents. This method also permits one to test for heterogeneity of the line and provides the means for approximating the confidence limits of doses other than the ED_{50}.

Although graphical solutions very often are adequate, the distribution of experimental points and their relative weights may be too irregular to place sufficient confidence in a line drawn visually. The exact probit solution obviates these difficulties by using a series of successive approximations, the first being given by the Kärber method.

The Kärber method gives simple nonparametric estimates of the mean and standard deviation of the distribution of critical levels. It is exceptionally useful when the mathematical form of the distribution is unknown, and it is a good initial estimate for iterative computational procedures. In addition, the method does not require a constant interval between successive dosages or a constant number of test sites at each dosage. Using this method, an equation of the regression line is established. To obtain the best fitting line several iterations are performed until the same equation is obtained for two successive iterations. This exact probit method, although the most precise, is quite complex and cumbersome to use without computer facilities.

Results

Ophthalmoscopic data. Threshold data were obtained using ophthalmoscopic criteria for exposure durations of 12, 70, 125, and 1,000 msec. Histograms were constructed using increments of 2 mw., staggered 1 mw. apart, to produce two overlapping step-functions. A typical histogram is shown in Fig. 3, and a summary of data based on the histograms appears in Table I. Included in Table I are the lowest powers at which damage was observed with the ophthalmoscope and the 50 per cent and estimated 0 per cent intercepts as obtained from the probability curves.

In the graphical probit method, increments of 2 mw. were used and the damage probability was plotted against the average power of the increment (Fig. 4). Table II lists the ED_{50}, $ED_{0.1}$, slope of the regression line, and the corresponding 95 per cent confidence intervals.

Exact probit solutions of the data were

Table I. Summary of data based on histograms

Pulse duration (msec.)	*No. of exposures*	*No. of eyes used*	*Lowest power* for observable damage (mw.)*	*50% damage probability (mw.)*	*Estimated 0% intercept (mw.)*
12	167	9	9	19.5	3.00
70	156	9	7	12.5	2.50
125	181	13	7	10.5	2.00
1,000	133	8	2	6.0	0.75

*Total power incident at the cornea.

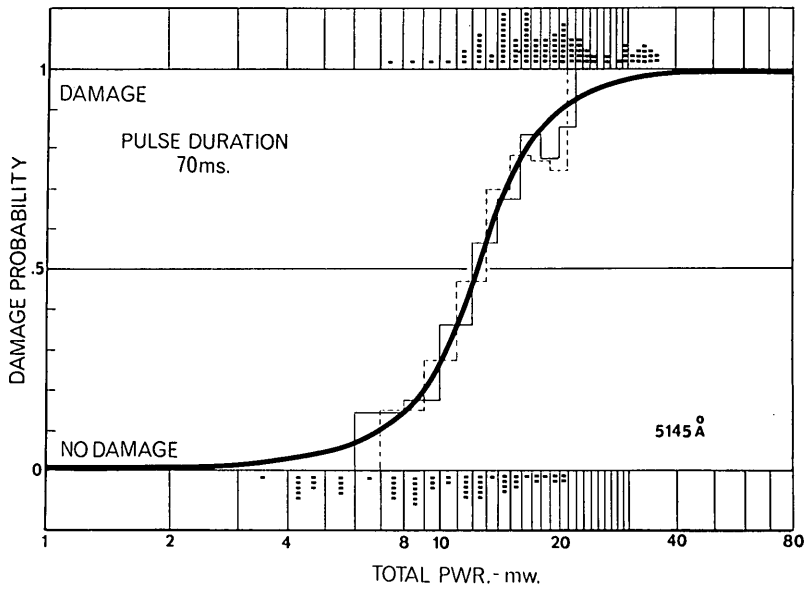

Fig. 3. Histogram of damage probability from argon laser (5,145 Å) at 70 msec. exposure.

computed using the Kärber method as the first approximation (Table III). A typical comparison of the graphical and exact probit solutions is shown in Fig. 5, where the line a-a′ represents the regression line as obtained from the graphical solution, while b-b′ is the line obtained through the exact probit method.

Histopathologic data. The minimal damage seen in the flat-preparations was char-

Table II. Summary of data based on the graphical probit method of solution

Pulse duration (msec.)	*No. of exposures*	*Power°*				*Slope*	*95% CI on slope*
		Ed_{50} *(mw.)*	*95% CI (mw.)*	$Ed_{0.1}$ *(mw.)*	*95% CI (mw.)*		
12	158	18.5	16.5-20.7	5.00	3.2-7.0	1.55	1.4-1.7
70	131	12.5	11.2-14.0	3.90	2.5-6.0	1.48	1.4-1.6
125	170	11.5	10.1-13.1	1.70	0.9-3.0	1.85	1.6-2.1
1,000	133	5.5	4.6- 6.7	.83	0.4-1.6	1.83	1.6-2.1

°Total power incident at the cornea.

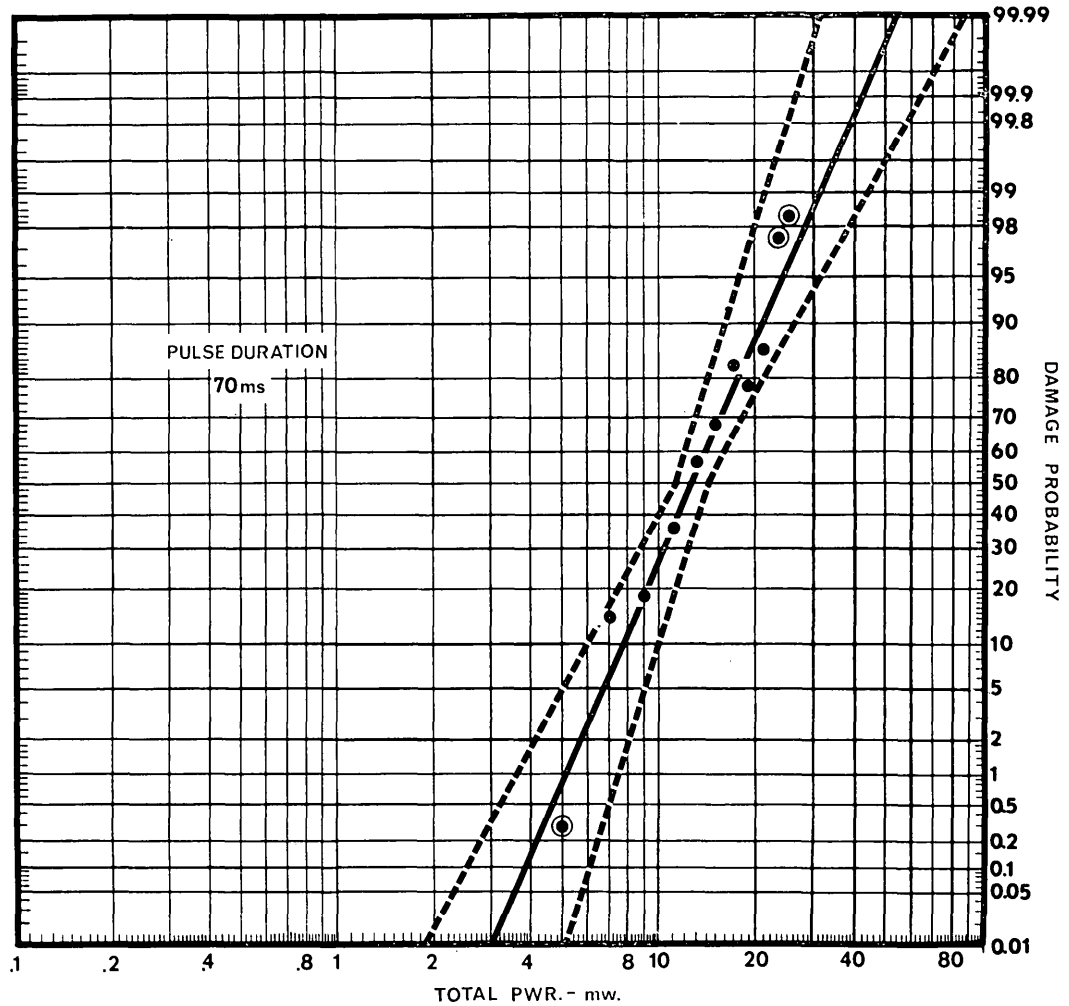

Fig. 4. Graphical probit solution of regression line and corresponding 95 per cent confidence intervals at 70 msec. exposure.

Table III. Summary of data based on the exact probit method of solution

Pulse duration (msec.)		*Power**		*Slope b-b'*
		Ed_{50} (mw.)	*Standard deviation*	
12	Kärber	17.1	1.4	1.65
	Final iteration	18.3	1.6	
70	Kärber	11.8	1.4	1.50
	Final iteration	11.8	1.5	
125	Kärber	11.8	1.5	1.94
	Final iteration	10.7	1.9	
1,000	Kärber	4.6	1.9	1.68
	Final iteration	5.0	1.7	

*Total power incident at the cornea.

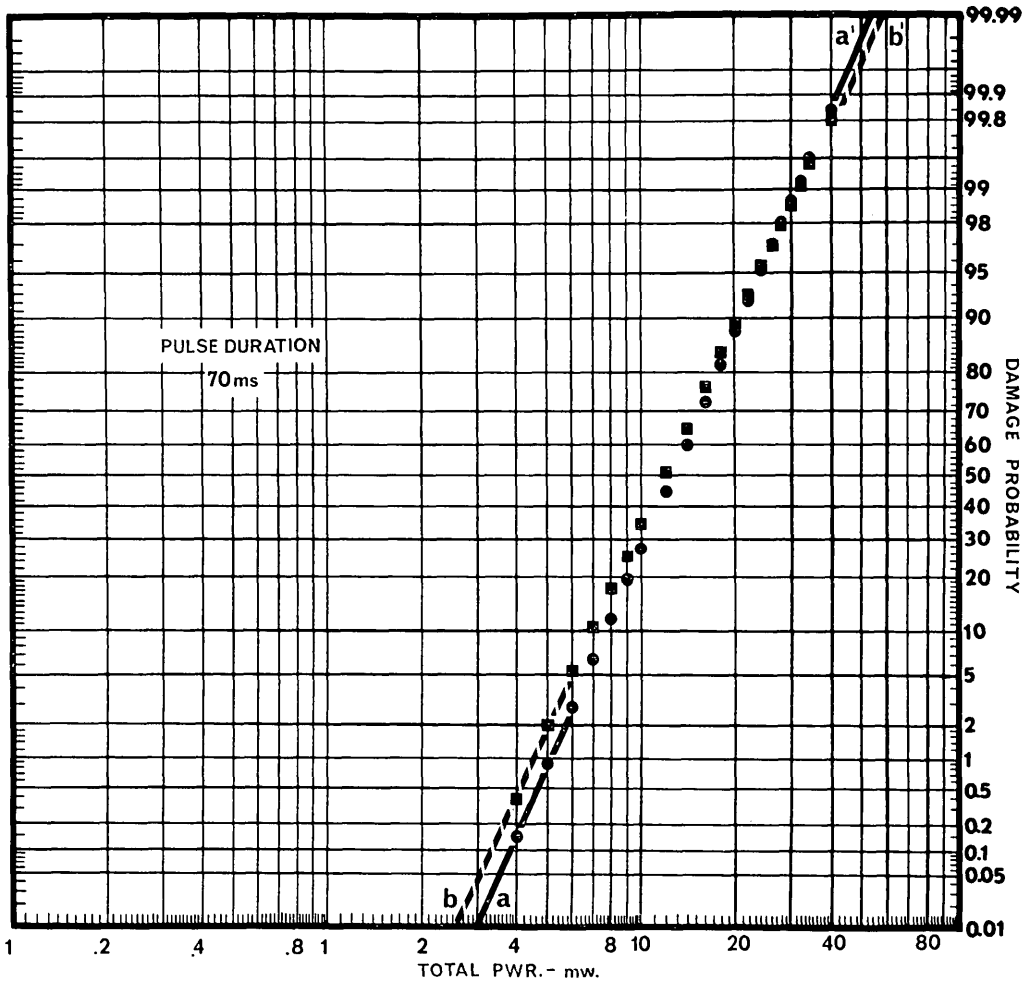

Fig. 5. Comparison of regression lines obtained through graphical (a-a') and exact (b-b') probit methods at 70 msec. exposure.

acterized by an area of pigment epithelial cell disruption and irregular pigmentation, measuring approximately 50 μ in diameter (Fig. 6). In serial sections examined up to three days after exposure, threshold damage consisted of swelling or disruption of the pigment epithelium and photoreceptors. In older lesions there was a variable amount of proliferation of pigment epithelial cells and migration of pigment-laden macrophages into the subretinal space (Fig. 7). Occasionally, pyknotic

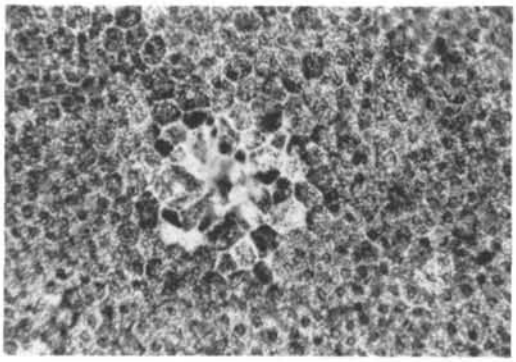

Fig. 6. Three-day-old retinal pigment epithelial lesion (Argon laser: 5,145 Å, 30 mw., 12 msec.). Note the cellular pleomorphism and irregular pigmentation. Unstained flat-preparation. (Hematoxylin and eosin. ×750.)

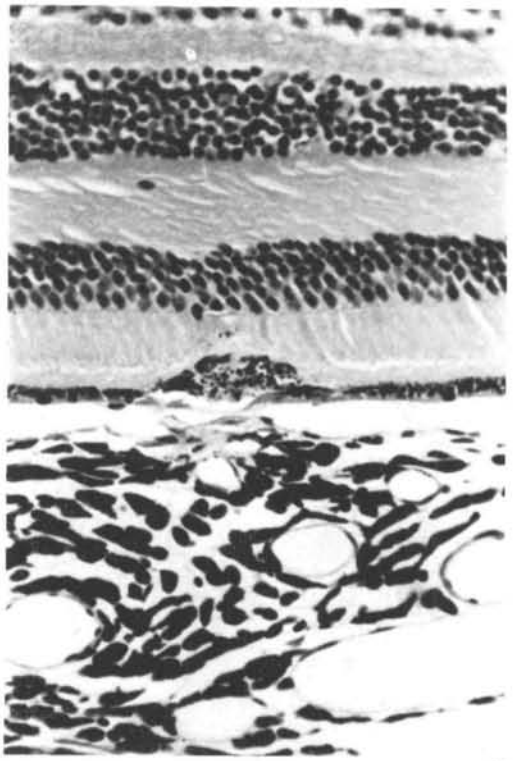

Fig. 7. Seven-day-old chorioretinal lesion (Argon laser: 5,145 Å, 24 mw., 12 msec.). Note the proliferation of pigment epithelium, photoreceptor damage and pathological changes in the choriocapillaris. (Hematoxylin and eosin. ×750.)

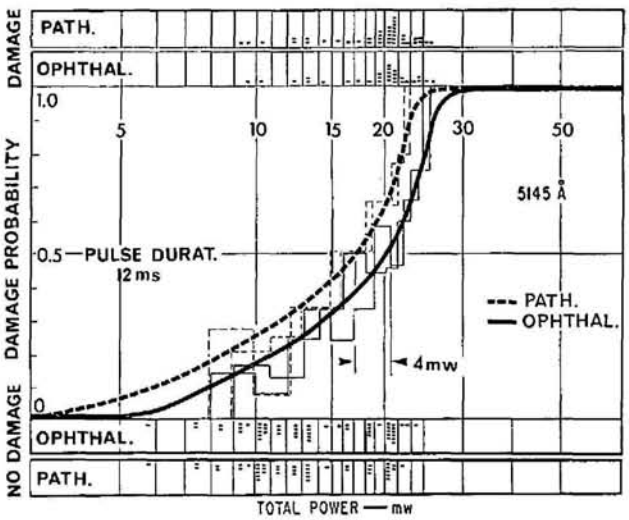

Fig. 8. Correlation between ophthalmoscopic and pathologic endpoints, presented in histogram form for 12 msec. exposure.

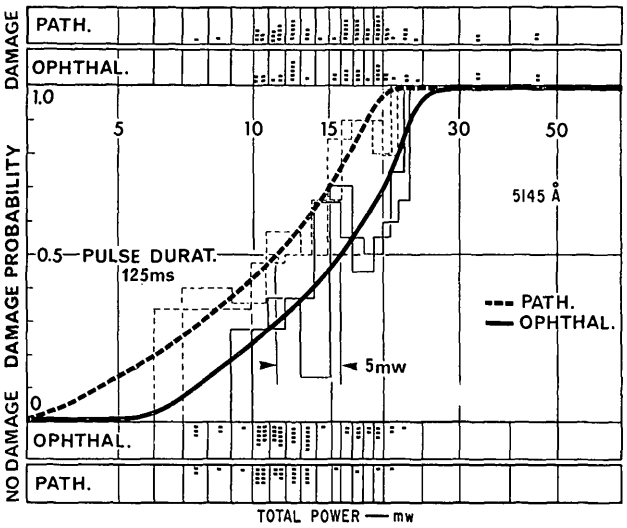

Fig. 9. Correlation between ophthalmoscopic and pathologic endpoints, presented in histogram form for 125 msec. exposure.

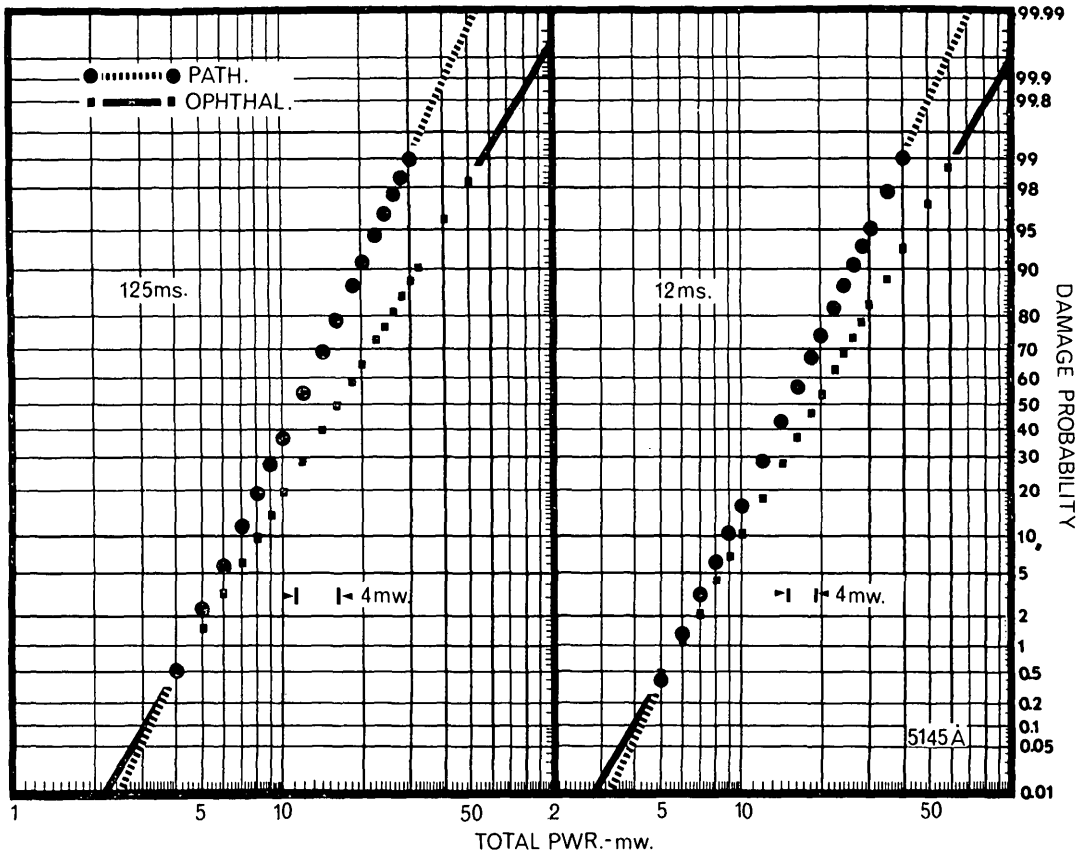

Fig. 10. Correlation between ophthalmoscopic and pathologic endpoints derived through exact probit method for 125 and 12 msec. Arrowed brackets denote difference of ED_{50} points.

Table IV. Correlation of data based on ophthalmoscopic versus pathologic endpoint

Pulse duration (msec.)	*No. of exposures*	*Damage criteria*	*Power**			*Slope*
			ED_{50} *(mw.)*	*Standard deviation*	ED_1 *(mw.)*	
12	81	Ophthalmoscopic	19.0	1.6	5.8	1.77
		Pathologic	15.0	1.5	5.7	1.65
125	84	Ophthalmoscopic	15.5	1.7	4.3	1.69
		Pathologic	11.5	1.5	4.6	1.52

*Total power incident at the cornea.

nuclei were found at the inner aspect of the outer nuclear layer. Damage to the sensory layers of the retina was never seen in the absence of pathologic changes in the pigment epithelium.

A comparison between ophthalmoscopic and histopathologic (flat-preparations) threshold data was undertaken for the 12 and 125 msec. pulse durations (Figs. 8, 9, and 10; Table IV). At both time durations the pathologic technique was consistently more sensitive.

Discussion

The hazard to the retina from argon laser radiation is related to both the transparency of the ocular media at the argon wavelengths and the inherent ability of the ocular refracting elements to focus the incident coherent light down to a small spot on the retina. In an attempt to simulate the "worst case" hazard conditions, our experimental system was designed to achieve a "minimal" retinal spot size by correcting the animal's refractive error and by using a narrow beam (1.6 mm.) of low divergence (0.7 milliradians) directed through the central portion of the cornea.

Argon threshold studies utilizing a similar exposure configuration have been reported by Vassiliadis and associates.[3] Extrapolation of their ophthalmoscopic data for 4.4, 13.5, and 80 msec. exposures (at 5,145 Å) shows good agreement with our ophthalmoscopic determinations for 12 and 70 msec. exposures.

Our laser system produced retinal damage sites as small as 50 μ in diameter. Jones and colleagues[9] concluded from theoretical considerations of the modulation transfer function of the eye that the ophthalmoscopic detection of retinal damage would be impaired for lesions less than 200 μ in diameter. In performing microscopic examinations of retinal flat-preparations, we eliminated the animal's refracting media and enhanced the resolution capabilities of the observer-system. This resulted in a 20 to 25 per cent reduction of our ophthalmoscopic estimate of the damage threshold at the ED_{50} point for the two exposure durations so investigated.

It is reasonable to assume that a similar reduction would be found at other exposure durations and probably for other laser systems where a "minimal" retinal spot configuration is utilized. One must take this into consideration when ophthalmoscopic data of this nature is used to define safe limits of ocular exposure to laser radiation.

Dr. Myron Yanoff assisted in the preparation and evaluation of the histopathologic material.

REFERENCES

1. L'Esperance, F. A., and Kelly, G. R.: The threshold of the retina to damage by argon laser radiation, Arch. Ophthal. 81: 583, 1969.
2. Taleff, M., Ritter, E. J., Rockwell, R. J., and Lotspeich, B. C.: Laser coagulation of the retina using the argon laser, Amer. J. Ophthal. 67: 666, 1969.
3. Vassiliadis, A., Rosan, R. C., and Zweng, H.

C.: Research on ocular laser thresholds, Final Report, Contract F41609-68-C-0041, SRI project 7191, Stanford Research Institute, Menlo Park, Calif. (August, 1969).

4. Vassiliadis, A., Rosan, R. C., Peabody, R. R., Zweng, H. C., and Honey, R. C.: Investigation of retinal damage using a Q-switched ruby laser, Special Technical Report, Contract AF33(615)-3060, SRI project 5571, Stanford Research Institute, Menlo Park, Calif. (August, 1966).
5. Leibowitz, H. M., Peacock, G. R., and Friedman, E.: The retinal pigment epithelium: radiation thresholds associated with the Q-switched ruby laser, Arch. Ophthal. **82**: 332, 1969.
6. Lappin, P. W., and Coogan, P. S.: Histologic evaluation of ophthalmoscopically subvisible retinal laser exposures, INVEST. OPHTHAL. **9**: 537, 1970.
7. Yanoff, M., Landers, M. B., and Bresnick, G. H.: Technique for flat-mount retinal pigment epithelial preparation, Ann. Ophth. In press.
8. Litchfield, J. T., and Wilcoxon, F.: A simplified method of evaluating dose-effect experiments, J. Pharm. Exp. Ther. **96**: 99, 1949.
9. Jones, A. E., Fairchild, D. D., and Spyropoulos, P.: Laser radiation effects on the morphology and function of ocular tissue, Second Annual Report, Contract No. DADA-17-67-C-0019, Honeywell, Inc. (July, 1968).